Analysis of dilatometer test in calibration chamber

Lech Bałachowski
Gdańsk University of Technology, Poland

Keywords: calibration chamber, DMT, quartz sand, FEM

ABSTRACT: Because DMT in calibration test chamber is two parameter test performed in well defined boundary conditions with a homogeneous soil mass, it presents an interesting possibility for numerical simulations. Insertion of the blade followed by membrane inflation was modeled. Dilatometer tests performed in calibration chamber at Gdańsk UT were modeled with finite element methods using Mohr-Coulomb and Hardening Soil Models. Soil data from triaxial tests were used to define model parameters. The tests made in loose and dense sand at different stress levels were modeled. The influence of BC1 and BC3 conditions and size effect in the calibration chamber was studied numerically. *A* and *B* values measured in dilatometer tests were compared to the calculated mean contact normal stress acting on the dilatometer membrane after the blade insertion and after the inflation of the membrane, respectively. Two modes for membrane inflation were applied: uniform horizontal stress and volumetric strain imposed. A more realistic shape of the membrane displacement and a better correlation with calibration chamber data were obtained with volumetric strain imposed. A good correlation was found between *A* and *B* values measured in calibration chamber and the calculated mean normal contact stress on the membrane.

1 DMT TESTS IN CALIBRATION CHAMBER

A series of dilatometer tests in the calibration chamber were performed for confining pressures ranging from 50 to 400 kPa with either loose or dense sands. The soil specimen was 53 cm in diameter and 100 cm high. The detailed description of the calibration chamber is given in Bałachowski and Dembicki (2000). Soil mass in the calibration chamber is prepared with sand raining. Dense soil mass (I_D=0,8) is obtained with stationary device. Soil mass with I_D=0,4 is formed using small traveling sieves and small falling height of grains. The sand mass is consolidated with K_0 conditions. Predominantly quartz uniform (U=1,4) fine sand (d_{50}=0,21 mm) from the Baltic beach in Lubiatowo is used. The sand parameters were obtained from triaxial CID tests for loose, medium dense and dense sand specimens. Maximum angle of internal friction ϕ_{max} (Fig. 1), modulus of deformation E_{50} at the half of deviatoric stress at failure (Fig. 2) and dilatancy angle ψ were determined. These parameters at given consolidation stress (here 50 kPa) are used (Table 1) to model the soil behavior using Mohr-Coulomb (M-C) and Hardening Soil Model (HSM).

A boundary condition with constant lateral stress (BC1) was maintained during blade insertion. At the end of each 5 cm step of penetration the membrane was inflated and *A* and *B* measurements were read. An example of readings taken at a vertical stress of 100 kPa applied to the upper membrane in the calibration chamber is given for loose and dense sand (Fig. 3). Quite uniform distribution of readings with depth is observed. Derived *A/B* ratio, up to 10, is typical for clean quartz sand.

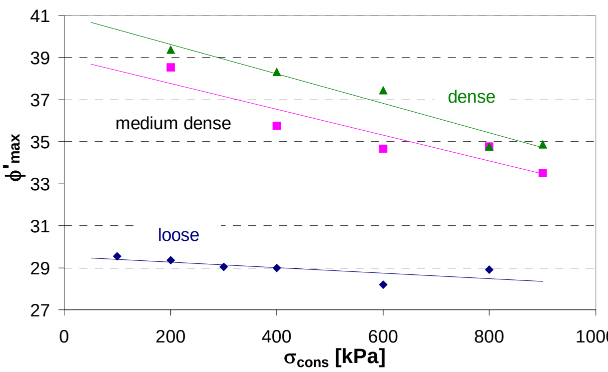

Figure 1. Angle of internal friction.

BACK

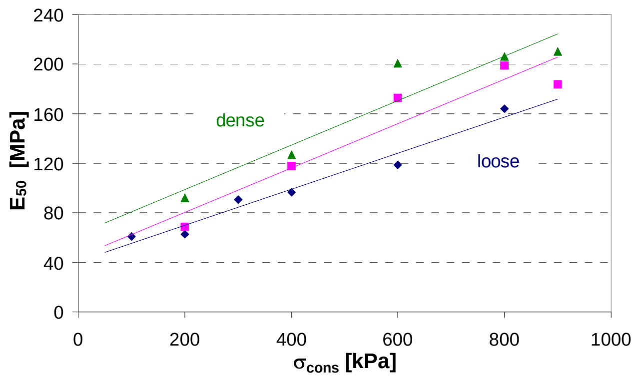

Figure 2. Modulus of deformation E_{50}.

Table 1. Soil parameters from triaxial tests.

I_D [-]	ϕ [°]	ψ [°]	E_{50} [MPa]
0,4	35	5	40
0,8	42	15	70

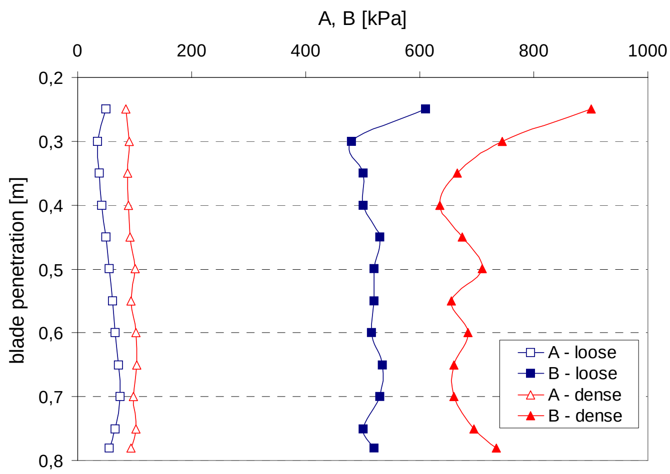

Figure 3. Profiles of A, B measurements in calibration chamber with σ'_v = 100 kPa.

2 NUMERICAL ANALYSIS

2.1 *Plain strain vs. axisymetric problem*

The penetration of dilatometer and the inflation of the membrane are very complex, truly three dimensional phenomena. The penetration of the dilatometer blade, being almost flat, can be considered in simplified manner as 2D problem. The inflation of the circular membrane is, however, a truly 3D phenomena.

Two schemes for membrane inflation analysis in elastic conditions can be considered (Fig. 4). In a first one – corresponding to plane strain conditions - membrane can be treated as a simple beam with free supports. In the second scheme circular plate with free supports on the circumference is considered.

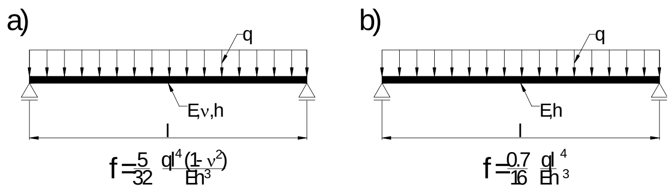

Figure 4. Schemes for membrane deflection: a) simple beam in plane strain conditions, b) circular plate

The formula for membrane deflection under uniform load for both schemes (Fig. 4) are given for :
- simple beam with ν=0,3 as :

$$f = 0{,}1422 \frac{ql^4}{Eh^3} \tag{1}$$

- circular plate as :

$$f = 0{,}0437 \frac{ql^4}{Eh^3} \tag{2}$$

For the same load, the membrane deflection will be thus about 3,5 times more important in plane strain conditions than in axisymetric ones. In order to model properly the inflation of circular membrane one should increase 3,5 times the imposed deflection of the membrane center for the calculation under plane strain conditions. The problem is however more complex as the soil is elasto-plastic and we should include not only the imposed pressure, but the soil response as well.

Some numerical analyses were done to verify the membrane response in plane strain and axisymetric conditions. The calculations were performed using PLAXIS v.8.2 code and Mohr-Coulomb (M-C) and Hardening Soil Model (HSM). A fine mesh, additionally refined near the blade and the membrane, with 15 nodes elements was used. The blade was placed horizontally on the surface of the box filled with sand. Due to symmetry only a half of the membrane was modeled. Vertical stress of 40 kPa was applied on the box surface to simulate lateral stress in the calibration chamber σ'_v = 100 kPa. Then the membrane was inflated by imposing volumetric strain in the cluster just behind the membrane. A numerical response corresponding to *B* reading was evaluated for plane strain (beam) and axisymetric conditions (circular plate). The computed contact normal stress distribution on the half of the membrane is given in Figure 5. Considerably higher contact normal stress is obtained for axisymetric conditions than for plane strain ones. Normal stress distribution is also given for the 1,1 mm displacement multiplied by 3,5 in plane strain conditions. Due to soil plasticity the contact normal stress in axisymetric case is higher than in plane strain conditions with 3,85 mm deflection at the membrane center.

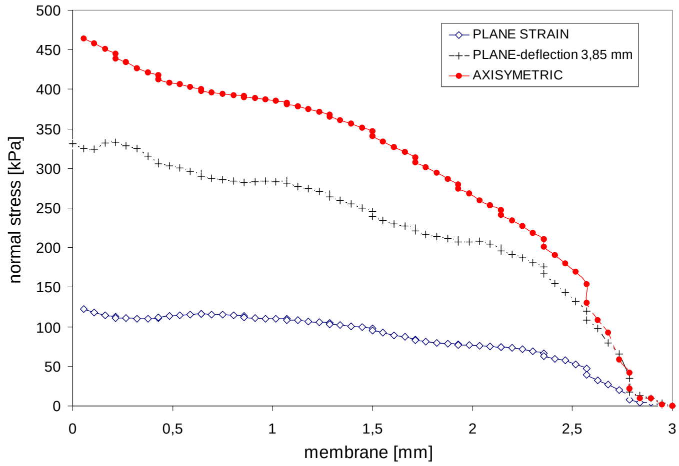

Figure 5. Calculated contact normal stress distribution on the dilatometer membrane.

2.2 *Modeling of blade insertion*

As a first approximation the real chamber dimensions were assumed for calculation mesh. The DMT blade was placed in the middle of the chamber. Stage calculations were made. Gravity was applied in addition to the boundary stresses and conditions. The blade shape was reproduced with the membrane 6 cm in diameter. An interface was introduced between the membrane and the soil. The penetration of the blade was stopped in the calculation when penetration resistance approaches asymptotic value. At this moment the normal stress distribution in the membrane interface was registered, which corresponds to *A* measurement. A series of preliminary calculations show that a considerable chamber size effect was observed during insertion phase (Fig. 6). Horizontal displacement fields after the blade insertion for the chamber of 53 cm and 200 cm in diameter are presented. For further analysis a chamber 200 cm in diameter was assumed.

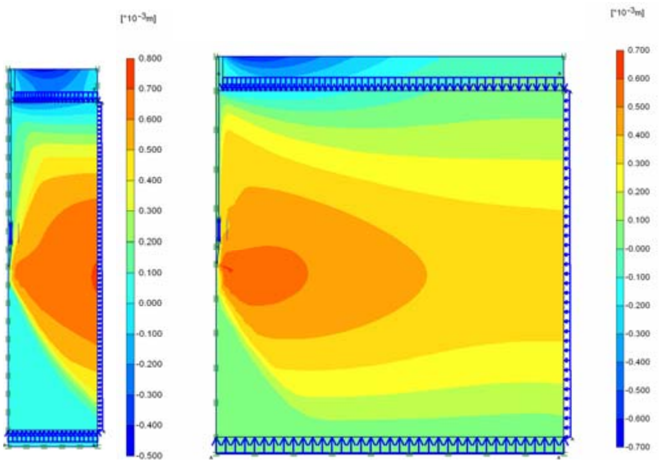

Figure 6. Horizontal displacement fields after the blade insertion for different diameter of the chamber.

2.3 *Modeling of blade inflation*

The membrane inflation was modeled in two manners (Fig. 7). According to the first one a cluster behind the membrane was inactivated and the lateral uniform stress was applied behind the membrane until its center was displaced 1,1 mm, corresponding to *B* measurement. Larger displacements at the edges of the membrane, related to the stress concentration, are observed than in the center (Fig. 8). Such a form of the membrane deflection is however unrealistic, so a different solicitation mode was considered. Moreover, as the membrane inflates the applied stress remains horizontal.

The membrane inflation was modeled with volumetric strain imposed in the cluster behind the membrane. The stress exerted on the membrane is not horizontal, but it is perpendicular to the membrane, which simulates the gas pressure. The maximum deflection of the membrane is observed in its center (Fig. 8). This mode of solicitation was chosen for further analysis.

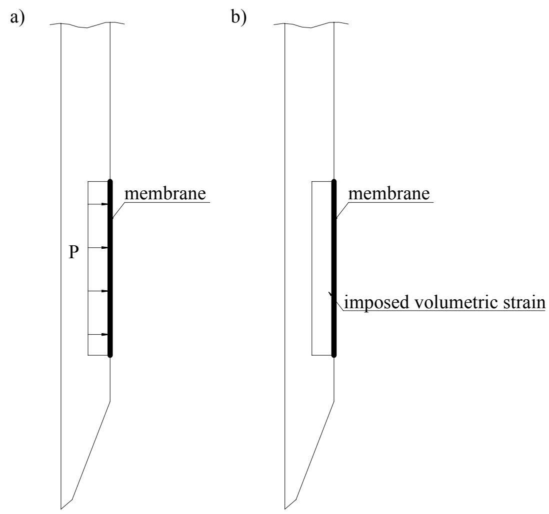

Figure 7. Two modes for membrane inflation.

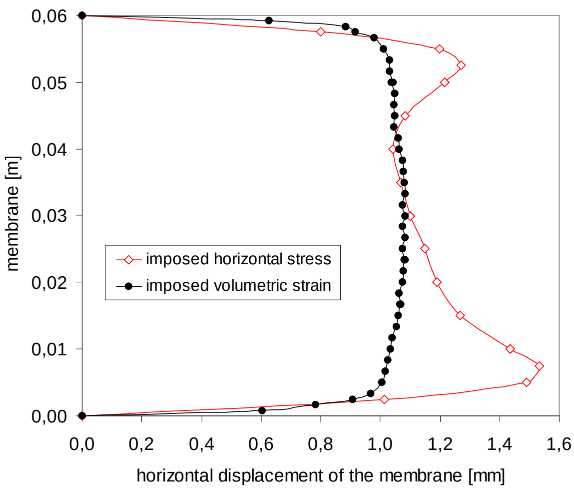

Figure 8. Shape of the inflated membrane with imposed horizontal stress and volumetric strain.

A considerable influence of chamber size effect can be found (Fig. 9) for the *B* measurement (inflated membrane). Chamber size effect in numerical analysis of normal stress distribution along the membrane corresponding to *A* and *B* measurements is given for dense sand (Fig. 10) and for loose sand (Fig. 11). Chamber radius of 100 cm minimizes the influence of the chamber size effect in the calculation. A calibration chamber 200 cm in diameter was used for further parametric studies.

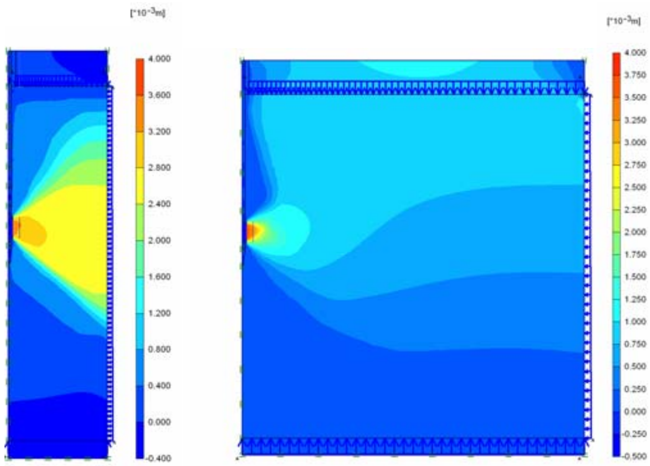

Figure 9. Horizontal displacement fields with inflated membrane.

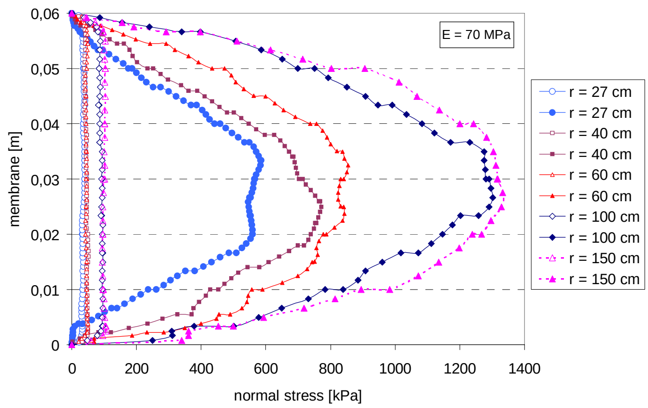

Figure 10. Normal contact stress on the membrane - chamber size effect for dense sand.

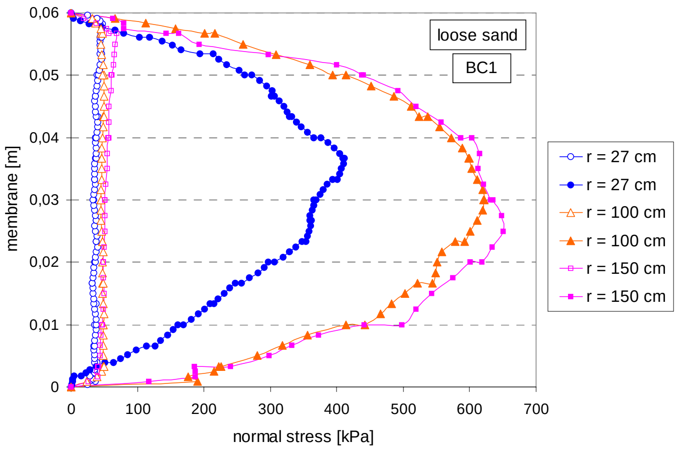

Figure 11. Normal contact stress on the membrane - chamber size effect for loose sand.

An influence of the soil modulus of deformation E_{50} on the calculated normal stress for *A* and *B* measurements was studied (Fig. 12). Calculations were performed for the angle of internal friction equal to 42. The calculated normal contact stress distribution on the membrane for *A* and *B* measurements is insensitive to soil modulus of deformation E_{50} higher than 70 MPa.

The contribution of the angle of internal friction was studied (Fig. 13) for dense sand with E_{50}=70 MPa. Contact normal stress to the membrane corresponding to *A* and *B* measurements is sensitive to the internal friction angle, especially for its high values.

The distribution of contact normal stress on the membrane for loose and dense sand is presented (Fig. 14) for the calculations performed with the soil parameters derived from triaxial tests. Mean contact normal stress on the membrane for loose and dense sand calculated with assumed soil parameters (Table 1) is given for dense sand (Table 2) and loose sand (Table 3). The evaluated mean contact stresses corresponding to both *A* and *B* measurements are close to the values measured in DMT test in calibration chamber (Table 2, Table 3).

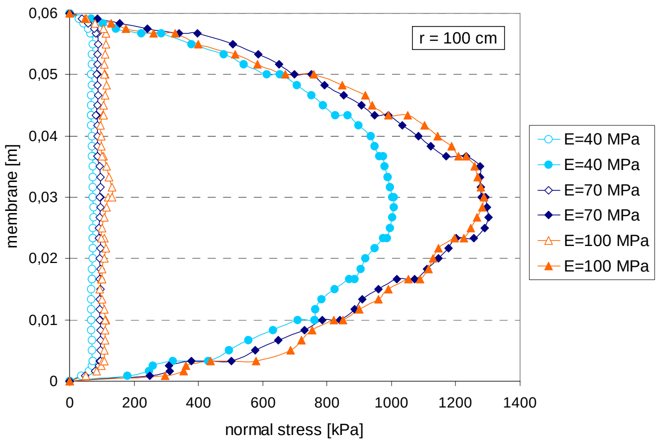

Figure 12. Normal contact stress on the membrane - influence of deformation modulus.

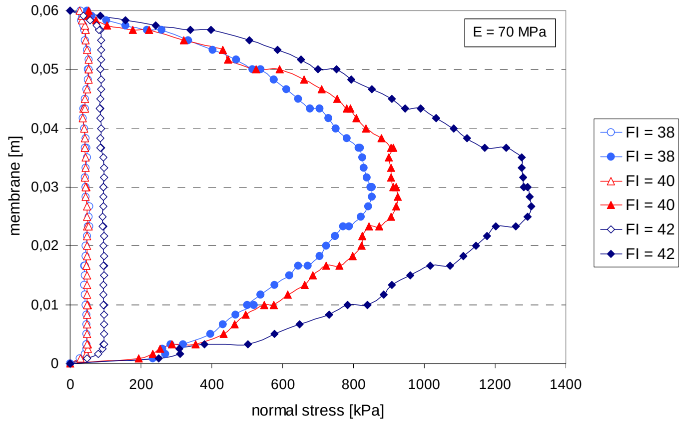

Figure 13. Normal contact stress on the membrane – influence of angle of international friction.

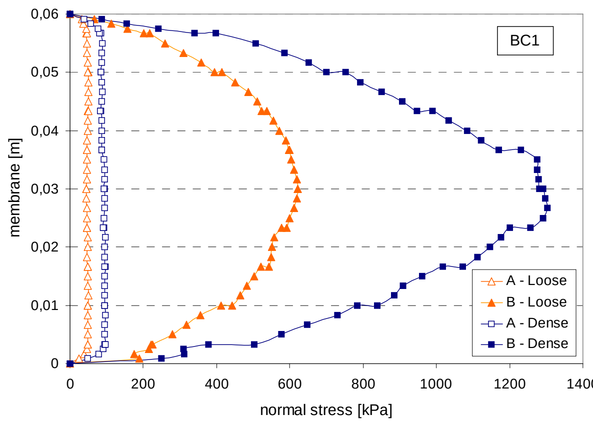

Figure 14. Normal contact stress on the membrane for loose and dense sand for *A* and *B* measurements.

Comparative analyses with M-C and HSM Soil Models were performed for dense sand using the same values of internal friction angle ϕ and modulus of deformation E_{50}. For *A* measurements the numerical analysis gives a similar response for both soil models. For membrane deflection analysis, HSM gives smaller normal contact stress than M-C (Fig. 15).

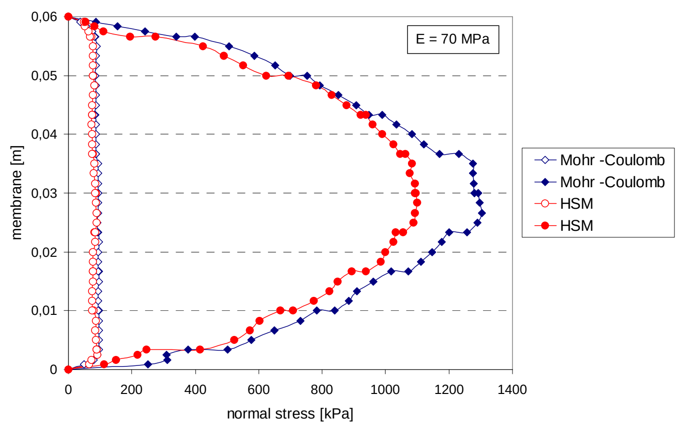

Figure 15. Normal contact stress on the membrane calculated for M-C and HSM soil models.

Table 2. Calculated mean normal contact stress to the membrane for dense sand.

E_{50} [MPa]	ϕ [°]	M-C		HSM	
		A [kPa]	B [kPa]	A [kPa]	B [kPa]
40	42	65	679	78	662
70	38	42	558		
	40	44	608		
	42*	85	831	76	721
100	42	101	858		

* A=92 kPa, B=670 kPa for DMT in calibration chamber

Table 3. Calculated mean normal contact stress to the membrane for loose sand.

E_{50} [MPa]	ϕ [°]	M-C	
		A [kPa]	B [kPa]
30	35	41	402
40	35#	45	427
	38	50	518
70	35	43	475

\# A=62 kPa, B=520 kPa for DMT in calibration chamber

2.4 *Influence of boundary conditions*

The comparison of the calculated distribution of normal contact stress at BC1 and BC3 boundary conditions is given for dense (Fig. 16) and loose sand (Fig. 17). Higher normal stress is calculated for no lateral strain condition (BC3) than at constant lateral stress (BC1) condition. The contribution of the boundary condition is more evident for dense sand.

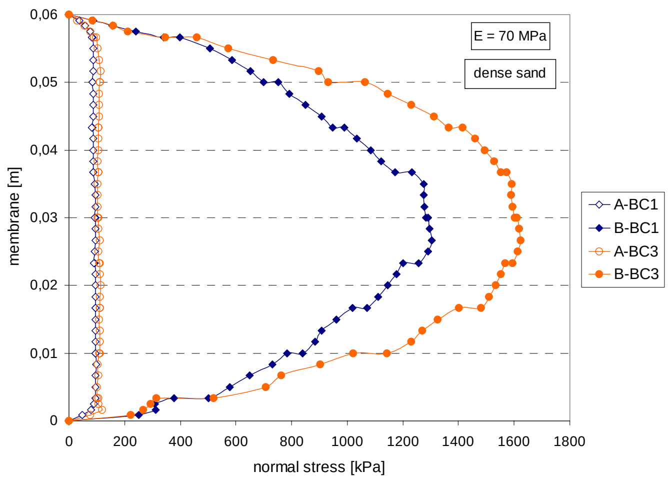

Figure 16. Normal contact stress on the membrane for BC1 and BC3 conditions for *A* and *B* measurements.

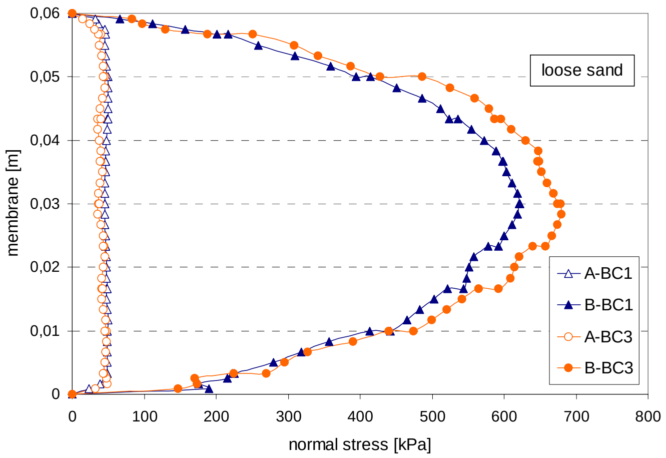

Figure 17. Normal contact stress to the membrane for BC1 and BC3 conditions for *A* and *B* measurements.

3 CONCLUSIONS

DMT model test with well defined boundary conditions in a reference sand was studied with FEM. Simplified two dimensional analysis in plane strain conditions were used to model 3D problem of blade insertion and membrane inflation. Larger deflection of the dilatometer membrane was applied in numerical analysis in order to adjust and approximate axisymetric response of circular membrane. A quite good approximation of DMT model tests was obtained in numerical modeling of two pressures (*A*, *B*), independently.

The parametric studies were performed and the analysis shows that the calculation performed with the soil parameters derived from triaxial tests fits well the measurements in calibration chamber. The results are sensitive to the internal friction angle and less to the modulus of deformation.

Sensitivity analysis shows that the chamber with at least 200 cm in diameter is necessary to minimize chamber size effect in numerical calculation. In reality the blade insertion induces less soil disturbance than in 2D case. Inflation of circular membrane generates less soil deformation than in plane strain conditions. It is generally considered that classical chamber 120 cm in diameter permits to avoid size effect in dilatometer tests. With the calibration chamber 53 cm in diameter some size effects could be however observed, especially for dense specimen.

Additional analyses are necessary to model the blade insertion with large deformation analysis. Analysis with PLAXIS code, even with updated mesh procedure, does not permit to reach large displacement during dilatometer blade insertion. Further research with 3D analysis is necessary.

ACKNOWLEDGEMENTS

I express my gratitude to prof. Silvano Marchetti for his suggestions and for supplying DMT equipment used in the calibration chamber tests.

REFERENCES

Baldi, G. Bellotti, R. Ghionna, V. Jamiolkowski, M. Marchetti, S. & Pasqualini, E. 1986. Flat dilatometer tests in calibration chambers. Proc. In Situ'86, GT Div., ASCE, June 23-25, Blacksburg, VA : 431-446.

Bałachowski, L. & Dembicki, E. 2003. La construction d'une chambre d'étalonnage à l'Université Technique de Gdańsk. Studia Geotechnica et Mechanica, Vol. XXV, No. 1-2.

Jamiolkowski, M. Lo Presti, D. C. F., Manassero, M. 2001. Evaluation of relative density and shear strength of sand from CPT and DMT. LADD Symposium, October 2001.

Marchetti, S. 1980. In situ tests by flat dilatometer, Journal of the Geotechnical Engineering Division, ASCE, Vol. 106, No. GT3.

Marchetti, S. Monaco, P. Totani, G. & Calabrese, M. 2001. The flat dilatometer test (DMT) in soil investigations. A report by the ISSMGE Committee TC16. Proc. IN SITU 2001, Bali, May 21.

PLAXIS v.8.2 manual

BACK